International Journal of Mathematics and
Computer Science, **14**(2019), no. 4, 975–992

Micropolar Nanofluid Flow in Vertical Stretched Surface with Thermophoresis Effect and Brownian Motion

Nosheen Feroz, Saeed Islam, Zahir Shah, Muhammad Farooq, Rashid Nawaz, Hakeem Ullah, Muhammad Suleman

Department of Mathematics
Abdul Wali Khan University
Mardan, 23200, KP, Pakistan

email: muhammadfarooq@awkum.edu.pk

(Received May 31, 2019, Accepted August 31, 2019)

Abstract

In this work, thermophoresis quantity and Brownian motion are the fundamental descriptions in micropolar nanofluid flow past a stretching surface within the sight of thermal radiation. Moreover, the Newtonian heat impact is viewed as predominant. A nonlinear system of differential equations is obtained by utilizing the nondimensional transformational parameter in the model that can be determined by the homotopy technique. Material parameters, conjugate parameters, Prandtl number, thermophoresis parameters, Brownian motion parameters, Lewis number, emission parameters, microrotation velocity, nanoparticle concentration, and surface resistance are significant places of interest which talk about transfer rates through charts and tables. Examination demonstrates that higher radiance values and Brownian motion parameters cause upgrade in heat and mass convection. Current graphs are reliable with computations of existing studies in the sense of limitations.

Key words and phrases: Stretching sheet, Brownian Motion, Thermophoresis Effect, Micropolar Fluid.
AMS (MOS) Subject Classifications: 76Mxx, 35Exx, 35Qxx.
ISSN 1814-0432, 2019, http://ijmcs.future-in-tech.net

1 Introduction

We are concerned with The Brownian motion parameter and thermophoresis in the micropolar nanofluids flow. Choi [1] was the pioneer researcher to initiate the theory of heat transfer improvement by dispersion of nanoscale rock solid elements. Water, oil, ethylene, and glycol are low thermal conductors. So they have low heat transfer potentiality as well. Researchers have worked a lot to improve the heat convection through a process of nanofluids. Lopez et al. [2] worked on thermal radiation based on MHD nanofluid. The Overcurrent entropy generation and convective boundary conditions pass through vertical microchannels. Farooq et al. [3] found the nonlinear thermal radiation characteristics in viscoelastic nanofluid flow. Hayat et al. [4] investigated attractive Carson nanofluid move through an expandable barrel in which temperature relied upon thermal conductivity. Khan et al. [5] suggested a neutral inclined magnetic fluid stagnation zone flow along nanofluid with variable viscosity and thermal radiation. Microstructured and unstable stretching capacity liquids are reported as micropolar liquids. The basic concept of polar liquids was first presented by Eringen [6,7]. After a short and condensed study, Lukaszewicz [8] introduced the use of micropolar fluids. As a matter of fact, the micropolar fluid shows that the disorderly fluid is interrupted in the viscous flow. Condensation of gemstones, body fluids, colorful emollients, colloidal suspensions, paints, and intense shear flow study are performed. Mohammedan and Gorla [9] first concentrated on a micropolar fluid with the help of a magnetic field gradient on a horizontal flat plate with mass transfer. Kasivishwanathan et al. [10] studied the MHD micropolar liquid flow and succeeded in gaining an accurate solution. Agarwal and Dhanapal [11] conducted a fact-finding study of the micropolar fluid flow of free convection inside parallel penetrable plates locating vertically with numerical alignment. Bhargava et al. [12] analytically examined the flow of mixed convective micropolar fluids on pores containing expanded sheet with a solution of a finite component. Nazar et al. [13] and Ishak et al. [14] worked on the stagnating point flow of micropolar fluids on the stretched surface. Ziabakhsh et al. [15] applied homotopy techniques to align and explore fluids with micropores in pores containing channels with mass and heat transfer. Srinivasacharya et al. [16] observed closely the insecure micropolar fluids between parallel plates and holy plates. Nadeem et al. [17, 18] analyzed micropolar nanofluids in two parallel plates with rotating properties. A reasonable solution to the problem was procured and the established specifications were considered in detail in the work. With

the demand for micropolar nano liquid use in an industrial area, it has multitudinous functions in pharmacopeia technology, hybrid motors, fuel cells, microelectronics. Wang et al. [19] expounded the invaluable idea about nanofluids. Their study was based on laboratory experiments and extensive discussion about its applications. One of the recognized problems is a nanofluid flow between parallel plates that accelerate MHD control generators. purification of crude petroleum, aerodynamic warming, oil manufacturing, spray and use of different vehicles Fluid. Metal has a tremendous application in terms of cooling frames. Goodman [20] examined the major discussion about viscous fluids in parallel flat plates. Borkakoti and Bharali [21] probed a hydromagnetic thick flow inside two parallel plates in which one is an extension plate. Attia et al. [22] considered the outcomes of viscous flow and magnetohydrodynamics between parallel plates. Sheikholeslami et al. [23-33] working, over the nanofluid flow of viscous liquid between parallel plates with steering frames, have explored in three measurements under the magnetohydrodynamic (MHD) effect. To master the unveiled complications, they applied a digital system and reported, in detail, the effect of non-dimensional guidelines on flow. Mahmoodi and Kandelousi [34] worked over the Magnetohydrodynamics consequences on kerosene-alumina nanofluidic flows in heat transfer research and Diverse modi operandi were put to use to solve the non-dimensional differential system deduced from the related model. Tauseef et al. [35] and Rokni et al. [36] considered the magnetohydrodynamic force and temperature gradient and the consequences of nanofluidic flow in parallel plates with steering frames. With the start of fluid's flow, the existing fluid particles rise and start rotating, because of its essential character, to a certain number of degree. Taylor and Geoffrey [37] shed light on the initiatory assessment of the motion of the viscous fluid typified in a rotation system. Greenspan [38] conducted the same analysis forward as the motion of the viscous fluid in a rotating system. Vajravelua and Kumar [39] examined the magnetohydrodynamic viscous fluid flow that existed in two plates having a pivotal and parallel position, in these one plate extends and the other has pores in it. They unearthed the numerical alignment and focused the property of physical criteria. Hayat et al. [40-41] exhibited the non-Newtonian fluid flow, applying an unusual model, by extending their work in two and three measurements. Non-Newtonian materials are also applied in industries including the manufacture of soft and elastic materials, oil-related goods, grease, paints, processed foods, and biological fluids. In such type of liquids, the connection between stress and strain is essentially non-linear.

2 Problem Formulation

A Two-dimensional incompressible micropolar nanofluid over a stretching surface has been considered. The stretching surface has a linear velocity $u_w(x) = cx$. In y direction of the fluid flow, the magnetic field is taken. At the surface T and T_∞ is the fluid flow temperature which is ambient from the surface. C and C_∞ are the surface deliberation and ambient from the surface. The impacts of thermal radiation, Newtonian heating, Brownian motion, and thermophoresis have been taken on the fluid flow phenomena. The governing equations for the fluid flow phenomena are as:

$$\frac{\partial u}{\partial x} + \frac{\partial v}{\partial y} = 0 \tag{2.1}$$

$$u\frac{\partial u}{\partial x} + v\frac{\partial u}{\partial y} = \left(v + \frac{k}{\rho}\right)\frac{\partial^2 u}{\partial y^2} + \frac{k}{\rho}\frac{\partial N}{\partial y} - \sigma B_0^2 u - g_r\beta_T(T - T_\infty) + g_r\beta_T(C - C_\infty), \tag{2.2}$$

$$u\frac{\partial N}{\partial x} + v\frac{\partial N}{\partial y} = \frac{\gamma^*}{\rho j}\frac{\partial^2 N}{\partial y^2} - \frac{k}{\rho j}\left(2N + \frac{\partial u}{\partial y}\right), \tag{2.3}$$

$$u\frac{\partial T}{\partial x} + \frac{\partial T}{\partial y} = \alpha_m\frac{\partial^2 T}{\partial y^2} + \frac{16\sigma^*}{3k^*}\frac{T_\infty^3}{\rho C_p}\frac{\partial^2 T}{\partial y^3} + \left(D_B\frac{\partial C}{\partial y}\frac{\partial T}{\partial y}\frac{D_T}{T_\infty}\left(\frac{\partial T}{\partial y}\right)^2\right) + q'', \tag{2.4}$$

$$u\frac{\partial C}{\partial x} + v\frac{\partial C}{\partial y} = D_B\frac{\partial^2 C}{\partial y^2} + \frac{D_T}{D_\infty}\frac{\partial^2 T}{\partial y^2}, \tag{2.5}$$

with boundary conditions

$$u = u_w(x) = cx, v = 0, N = -n\frac{\partial u}{\partial y}, \frac{\partial T}{\partial y} = -h_s T, C = C_w \tag{2.6}$$

at $y = 0, u \to 0, N \to 0, T \to T_\infty, C \to C_\infty$, as $y \to \infty$.
On top of equations u and v are considered components of velocity along x and y directions respectively. N is the microrotation, k is the vortex viscosity, T is the temperature, kI is the thermal conductivity, D_B is the Brownian diffusion, Rd is the Radiation parameter, D_T is the thermophoretic diffusion, T_∞ is the ambient temperature, C is the concentration, C_∞ is the ambient concentration, N_t is the thermophoresis parameter, N_b the Brownian motion parameter, L_e is the Lewis number, P_r is the Prandtl number, k is the micropolar parameter, V is the kinematic viscosity, q is the source/sink non-uniform term and is expressed as:

$$q''' = \frac{kU_w(x,t)}{xv}[A(T_w - T_\infty)f' + (T - T_\infty)B] \tag{2.7}$$

The similarity variables are defined as

$$\eta = y\sqrt{\frac{V}{\nu}}, u = Cxf'(\eta), N = \sqrt{\frac{C}{\nu}}Cxg(\eta), \nu = -\sqrt{C\nu}f(\eta), \theta(\eta) = \frac{T-T_\infty}{T_w-T_\infty}, \theta(\eta) = \frac{C-C_\infty}{C_w-C_\infty} \tag{2.8}$$

Using these similarity variables, equations (2-7) reduce to:

$$(1+K_1)F'' + FF'' - F'^2 - MF' + G_m\theta - G_r\phi = 0 \tag{2.9}$$

$$\left(1+\frac{K_1}{2}\right)G'' + FG' - F'G - 2k_1G - k_1F'' = 0 \tag{2.10}$$

$$\left(1+\frac{4}{3}R_d\right)\theta'' + P_r(F\theta' + N_b\phi'\theta' + N_t\theta'^2 + A_1F' + B_1\theta) = 0 \tag{2.11}$$

$$\phi'' + P_rL_eF\phi' + \frac{N_t}{N_b}\theta'' = 0 \tag{2.12}$$

satisfies the following the boundary conditions

$$f(0) = 0, f'(0) = 1, f'(\infty) \to 0, g(0) = -nf''(0), g(\infty) \to 0, \theta'(0) = -\gamma[1+\theta(0)], \tag{2.13}$$

$\theta(\eta) \to 0, \phi(0) = 1, \phi(\infty) \to 0.$

$$\alpha_m = \frac{k_1}{\rho C_p}G_m = (1-C_\infty)\rho_f B(T_w-T_\infty)g, G_r = (\rho_p-\rho_f)g(C_w-C_\infty), K_2 = \frac{\gamma^*}{\rho j\nu}, K_3 = \frac{2K}{\rho jc},$$

$A_1 = \frac{kU_wA}{x\nu c}, B_1 = \frac{kU_\infty B}{x\nu c}.$

In equations (10-13), $K_1 = \frac{k}{\rho\nu}$ depicts micropolar parameter,$M = \frac{\delta B_0^2}{c}$ represents magnetic parameter, $L_e = \frac{\alpha_m}{D_B}$ is the Lewis number, $\gamma = h_s\sqrt{\frac{\nu}{C}}$ indicates the conjugate parameter, $N_t = \frac{\tau D_T}{T_\infty\nu}$ represents thermophoresis parameter, $N_b = \frac{\tau D_B(C_w-C_\infty)}{\nu}$ indicates the Brownian motion parameter, $P_r = \frac{\nu}{\alpha_m}$ represents the Prandtl number, $R_d = \frac{4\sigma^*T_\infty^3}{k^*k_1}$ indicates the thermal radiation parameter.

3 Physical Quantities

Skin friction related to the problem is defined as $C_f = (\frac{S_{xy})_{y=0}}{\rho u_w^2}$

with $S_{xy} = (\mu+k)\frac{\partial u}{\partial y} + kN$. Nusselt number is defined as $N_u = \frac{hQ_w}{\hat{k}(T_0-T_h)}$ Q_w shows heat flux where $-\hat{k}\left(\frac{\partial T}{\partial y}\right)_{y=0}$. The Sherwood number is defined

as $sh = \frac{hJ_w}{D_B(C_0-C_h)}$ where J_w is the mass flux and defined as $J_w = -D_B = \left(\frac{\partial C}{\partial y}\right)|_{y=0}$. The dimensionless form of Skin friction, Nusselt number and Sherwood number respectively C_f, Nu and Sh are expressed as:

$$C_f = \frac{\tau_w}{\rho u_w^2},\ Nu_x = \frac{xq_w}{k_1(T-T_\infty)}, Sh_x = \frac{xq_m}{D_B(C_w - C_\infty)}, \tag{3.14}$$

where

$$\tau_w = \left[(\mu+k)(\frac{\partial u}{\partial y}) + kN\right]_{y=0},\ q_w = -\left[k_1 + \frac{16\sigma^* T_\infty^3}{3k^*}\right]\left(\frac{\partial T}{\partial y}\right)_{y=0},\ q_m = -D_B\left(\frac{\partial C}{\partial y}\right)_{y=0}. \tag{3.15}$$

Substituting equation (15) into (14), the equations for skin fraction coefficient and local Nusselt number reduce to

$$C_f Re_x^{\frac{1}{2}} = (1+(1-n))f''(0), \tag{3.16}$$

$$\frac{Nu_x}{Re_x^{\frac{1}{2}}} = \gamma\left(1+\frac{1}{\theta(0)}\right)\left(1+\frac{4}{3}R_d\right), \frac{Sh_x}{Re_x^{\frac{1}{2}}} = -\phi'(0), \tag{3.17}$$

where $Re_x = \frac{cx^2}{\nu}$ indicates the local Reynolds number.

4 Results and Discussion

In Fig. 1 the sway of Gm on velocity field $f'(\zeta)$ is accessible along x and y directions. The Gm velocity will increase with the velocity distribution $f'(\zeta)$ directly varies as Gm escalating in the x direction. In Fig. 2 we notice what will be the influence of Gr on velocity field $f'(\zeta)$ along x and y directions. The Gr velocity will increase with the velocity distribution $f'(\zeta)$ directly varies as Gr an increase in the x direction. The influence of K_1 on velocity field $f'(\zeta)$ along x and y directions is shown in Fig. 3. With an increase of K_1 in x direction the velocity distribution $f'(\zeta)$ directly varies. The velocity will increase by increasing K_1. That effect of magnetic parameter M on velocity field along with x and y directions is shown in Fig. 4. The velocity $f'(\zeta)$ decreases with an increase in M. That decrease in $f'(\zeta)$ occurred when we moved along the x axis then straight change in velocity profile $f'(\zeta)$ will occur in the y direction. Owing to the enrichment of the magnetic parameter M, when the fluid is local to the plates the velocity profile is decreasing, but this action is conflicting when M is acting along the y

direction. The enormity of a magnetic parameter M over the velocity field is that with the grow in M increases the force of friction of the movement is known as Lorentz force due to which decrease in the limit sheet the fluid velocity decreases, while another force recognized as Carioles force demonstrate the incongruous influence on the velocity next to the y direction. In Figs. 5 the characteristics of thermal conductivity KI on Momentum along x and y directions have been showed. From the mathematical formulation, it is clear that the momentum $G(\zeta)$ is negatively affected within the x direction and y-direction, that is openly changed with $G(\zeta)$. What will be the effect of magnetic parameters M on the momentum $G(\zeta)$ in the x and y directions that are shown in Figure 6. From the mathematical formula, it is clear that the velocity distribution $G(\zeta)$ is positively correlated within the x direction and negatively in the y direction. Magnetic parameters M and the momentum $G(\zeta)$ are directly proportional as with the increase in M, the momentum will also increases when approaching the board, but this action is reversed when acting in the y direction. The effect of the micro-rotation profile showed in Figure 6. The micro-rotation profile between the parallel plates will improve if the magnetic parameter is greater than before. The sway of n on Momentum $G(\zeta)$ along with x and y directions are shown in Figs. 7. Due to the mathematical formulation, that the momentum $G(\zeta)$ has reverse relation with n along x axis and direct relation with n along y axis. The uniqueness of $A1$ Heat transfer $\theta(\zeta)$ along the x and y directions are shown in Figs. 8. According to the mathematical formulation the Heat transfer $\theta(\zeta)$ is negatively changed with $A1$ along the x direction and positively changed with $A1$ along the y direction. In Figs. 9 the distinctiveness of $B1$ Heat transfer $\theta(\zeta)$ are illustrated along with x and y directions. From the mathematical formulation, it is clear that the Heat transfer $\theta(\zeta)$ negatively changes with $B1$ along the x direction and positive changes $A1$ along the y-directions. By Fig. 10 the influence of Nb on Heat transfer $\theta(\zeta)$ along with x and y directions is shown. From the mathematical formulation, it is clear that the Heat transfer $\theta(\zeta)$ is positively changed with Nb along the x direction and negatively changes with $\theta(\zeta)$ along the y direction. By Fig. 11 the manipulate of the thermophoresis parameter Nt on Heat transfer $\theta(\zeta)$ along x and y directions are shown. The mathematical formulation cleared that the Heat transfer $\theta(\zeta)$ positively changes with Nt along the x direction and negatively changes with $\theta(\zeta)$ along the y directions. In Fig. 12 The distinctiveness of Pr Prandtl number on Heat transfer $\theta(\zeta)$ along with x and y directions is illustrated. By the mathematical formulation, it is obvious that Heat transfer $\theta(\zeta)$ negatively changes with Pr Prandtl number along the x

direction and positively change with $\theta(\zeta)$ along the y direction. In Fig. 11 the manipulate of Rd Radiation parameter on Heat transfer $\theta(\zeta)$ along x and y directions is illustrated. From the mathematical formulation, it is obvious that Heat transfer $\theta(\zeta)$ positively changes with Rd along the x direction and negatively changes with $\theta(\zeta)$ along the y direction. By Fig. 14 the distinctiveness of Lewis number Le on deliberation field $\theta(\zeta)$ are illustrated along with x and y directions. From mathematical formulation, we observe that the concentration field $\theta(\zeta)$ will negatively be changed with Le along the x direction and positively changed with $\theta(\zeta)$ along the y direction. In Figure 15 the features of Nb (Brownian motion parameter) over $\theta(\zeta)$ (concentration field) along x and y directions are shown.By the mathematical formulation that is clear that the concentration field $\theta(\zeta)$ along the x direction will change negatively with Nb and along the y direction positively changes with $\theta(\zeta)$. In Fig. 16 the manipulate of thermophoresis Nt on the concentration field $\theta(\zeta)$ along with x and y directions are shown. By the mathematical formulation, we observe that the concentration field $\theta(\zeta)$ in the x direction is positively changing with Nt and with $\theta(\zeta)$ along the y direction negatively changes. In Fig. 17 the manipulate of Prandtl constant Pr over field concentration $\theta(\zeta)$ with x and y directions are demonstrated. From the mathematical formulation, it is clear that the concentration field $\theta(\zeta)$ along the x direction is positively changing with Pr and along the y direction negatively changes with $\theta(\zeta)$.

K_1	M	Gm	Gr	$CfRe_x^{1/2}$
0.1	0.1	0.1	0.1	1.049010
0.2				1.006290
0.3				0.968499
	0.1			1.049010
	0.2			1.090230
	0.3			1.130350
		0.1		1.049010
		0.2		1.042160
		0.3		1.029960
			0.1	1.049010
			0.2	1.099730
			0.3	1.150600

Table 1. Numerical values of skin friction coefficient for different dimensionless embedded parameters.

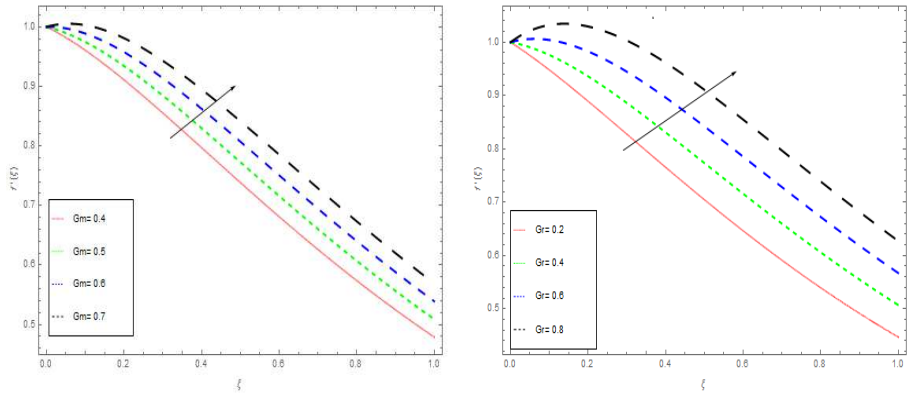

Figure 1: Influence of Gm over velocity profile $f'(\zeta)$, when $Pr = 0.5$,$Le = 0.4$,$N_t = 1$,$N_b = 0.6$,$M = 0.4$,$R_d = 0.7$,$n = 0.1$

Figure 2: Influence of Gr over velocity profile $f'(\zeta)$, when $Pr = 0.5$,$Le = 0.4$,$N_t = 1$,$N_b = 0.6$,$M = 0.4$,$R_d = 0.7$,$n = 0.1$

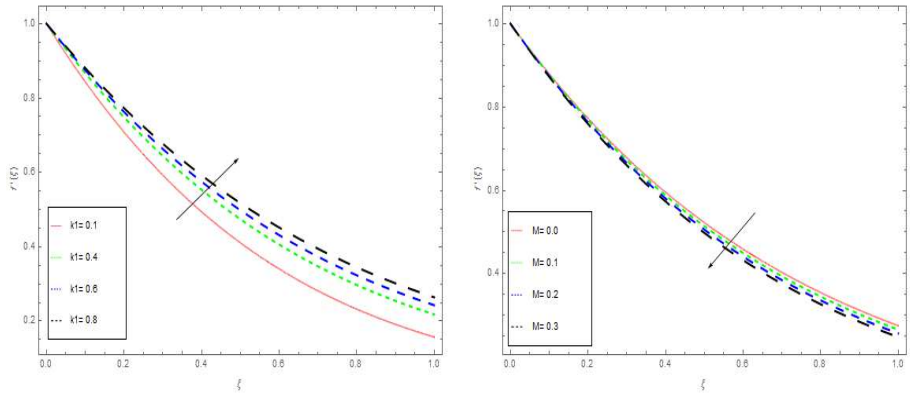

Figure 3: Influence of K_1 over velocity profile $f'(\zeta)$, when $Pr = 0.5$,$Le = 0.4$,$N_t = 1$,$N_b = 0.6$,$M = 0.4$,$R_d = 0.7$,$n = 0.1$

Figure 4: Influence of M over velocity profile $f'(\zeta)$, when $Pr = 0.5$,$Le = 0.4$,$N_t = 1$,$N_b = 0.6$,$K = 0.5$,$R_d = 0.7$,$n = 0.1$

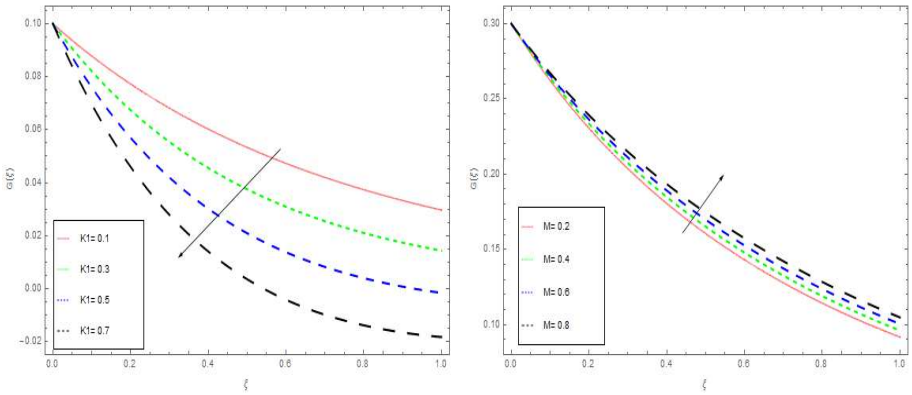

Figure 5: Influence of $K1$ over velocity profile $f'(\zeta)$, when $Pr = 0.5$,$Le = 0.4$,$N_t = 1$,$N_b = 0.6$,$M = 0.4$,$R_d = 0.7$,$n = 0.5$,$\gamma = 0.5$

Figure 6: Influence of M over velocity profile $G(\zeta)$, when $Pr = 0.5$,$Le = 0.4$,$N_t = 1$,$N_b = 0.6$,$K = 0.1$,$R_d = 0.7$,$n = 0.3$,$\gamma = 0.5$

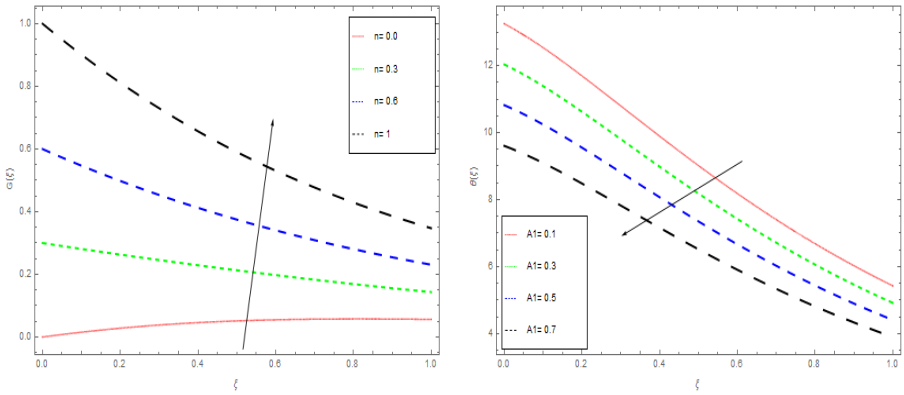

Figure 7: Influence of n over velocity profile $G(\zeta)$, when $Pr = 0.5$,$Le = 0.4$,$N_t = 1$,$N_b = 0.6$,$M = 0.4$,$R_d = 0.7$,$K = 0.5$,$\gamma = 0.1$

Figure 8: Influence of $A1$ over velocity profile $\theta(\zeta)$, when $Pr = 0.5$,$Le = 0.4$,$N_t = 1$,$N_b = 0.3$,$M = 0.4$,$R_d = 0.2$,$\gamma = 0.5$

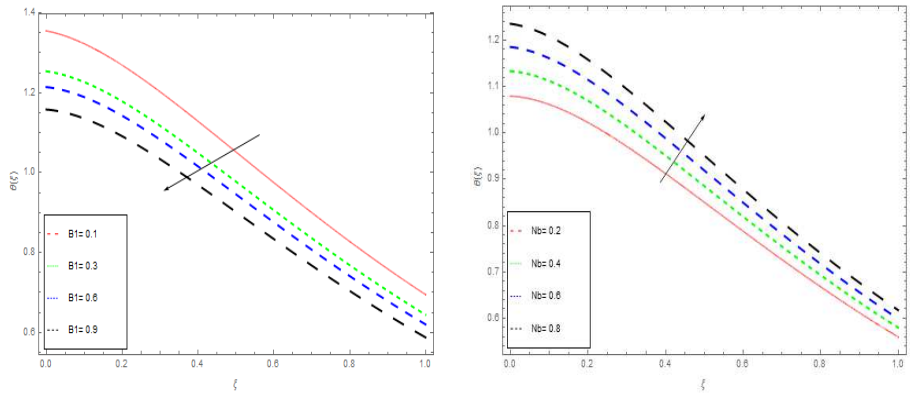

Figure 9: Influence of $B1$ over velocity profile $\theta(\zeta)$, when $Pr = 0.5$,$Le = 1$,$N_t = 1$,$N_b = 0.3$,$M = 0.4$,$R_d = 0.2$,$\gamma = 0.5$,$n = 0.1$

Figure 10: Influence of Nb over velocity profile $\theta(\zeta)$, when $Pr = 0.3$,$Le = 1$,$N_t = 0.1$,$M = 0.4$,$R_d = 0.3$,$\gamma = 0.5$,$n = 0.1$

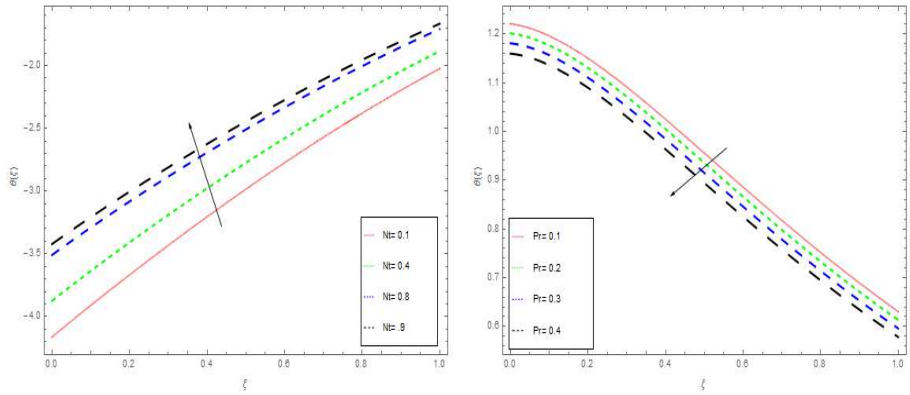

Figure 11: Influence of thermophoresis parameter Nt over velocity profile $\theta(\zeta)$, when $Pr = 0.3$,$Le = 1$,$N_b = 0.1$,$M = 0.4$,$R_d = 0.5$,$\gamma = 0.5$,$n = 0.5$

Figure 12: Influence of Pr Prandtl number on Heat transfer $\theta(\zeta)$, when $n = 0.1$,$Le = 1$,$N_t = 0.1$,$N_b = 0.6$,$M = 0.4$,$R_d = 0.3$,$\gamma = 0.5$

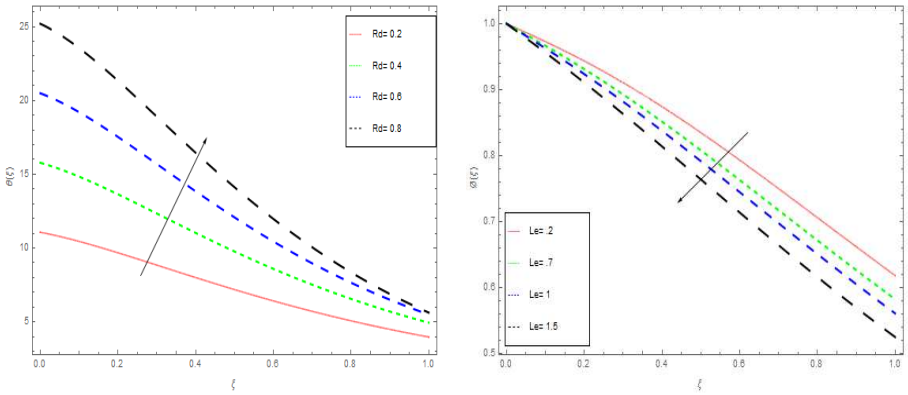

Figure 13: Influence of Rd Radiation parameter on Heat transfer $\theta(\zeta)$, when $Pr = 0.5$ $n = 0.1$,$Le = 0.4$,$N_t = 1$,$N_b = 0.6$,$M = 0.4$,$\gamma = 0.5$

Figure 14: Influence of Lewis number Le on concentration field $\phi(\zeta)$, when $Pr = 1$ $n = 0.5$,$Rd = 0.6$,$N_t = 0.4$,$N_b = 0.6$,$M = 0.4$,$\gamma = 0.5$

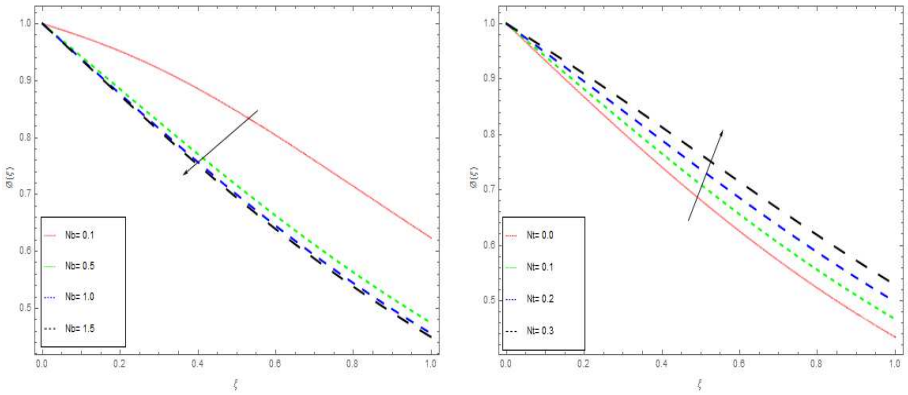

Figure 15: Influence of Brownian motion parameter N_b over the concentration field $\phi(\zeta)$, when $Pr = 1$ $n = 0.5$,$Rd = 0.3$,$N_t = 0.1$,$Le = 1.0$,$M = 0.4$,$\gamma = 0.5$

Figure 16: Influence of thermophoresis N_t on the concentration field $\phi(\zeta)$, when$Pr = 1$ $n = 0.5$,$Rd = 0.3$,$N_b = 0.6$,$Le = 1.0$,$M = 0.4$,$\gamma = 0.5$

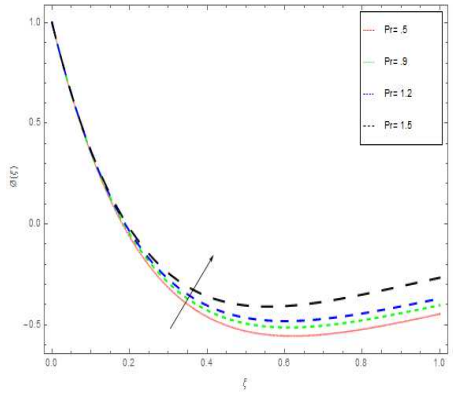

Figure 17: Influence of Prandtl number Pr on concentration field $\phi(\zeta)$, when$N_t = 0.4$ $n = 0.5$,$Rd = 1$,$N_b = 0.6$,$Le = 1.0$,$M = 0.5$,$\gamma = 0.5$

$A1$	$B1$	N_b	N_t	Pr	Rd	$NuRe_x^{1/2}$
0.1	0.1	0.1	0.1	0.1	0.1	0.1
0.2						0.437050
0.3						0.434774
	0.1					0.432498
	0.2					0.437050
	0.3					0.437071
		0.1				0.437093
		0.2				0.437050
		0.3				0.439715
			0.1			0.440604
			0.2			0.437050
			0.3			0.431721
				0.1		0.426412
				0.2		0.437050
				0.3		0.436455
						0.435846
					0.1	0.347050
					0.2	0.437419
					0.3	0.437558

Table 2. Numerical values of local Nusselt number for different dimensionless embedded parameters.

5 Conclusion

This study is performed to analyze the Radiative micropolar flow in vertical stretched surface with Brownian motion and thermophoresis effect. The main features are as follows

- The velocity function purges with the escalation in Gm, K_1, Gr while it decreases with the escalation in M.
- The momentum function $G(\zeta)$ is decreased with the increasing K_1, while increased with the escalation in M and n.
- Function of the heat transfer $\theta(\zeta)$ decreases with the escalation in Pr, $A1$ and $B1$ while increases with the escalation in N_b, N_t and Rd.
- Deliberation field $\theta(\zeta)$ is reduced with the escalation in and Le, N_b while increased with the escalation in N_t and Pr.

References

[1] Stephen U. S. Choi, Enhancing thermal conductivity of fluids with nanoparticles developments and applications of non-Newtonian fluid flow, ASME Fed. **66,** (1995), 99–105.

[2] A. Lopez, G. Ibanez, J. Pantoja, J. Moreira, O. Lastres, Entropy generation analysis of MHD nanofluid flow in a porous vertical microchannel with nonlinear thermal radiation, slip flow and convective-radiative boundary conditions, Int. J. Heat Mass Transfer, **107,** (2017), 982–994.

[3] M. Farooq, M. I. Khan, M. Waqas, T. Hayat, A. Alsaedi, M. I. Khan, MHD stagnation point flow of viscoelastic nanofluid with non-linear radiation effects, J. MolLiq, **221,** (2016), 1097-1103.

[4] T. Haya, M. I. Khan, M. Waqas, T. Yasmeen, A. Alsaedi, Viscous dissipation effect in the flow of magneto nanofluid with variable properties, J. Molliq, **222,** (2016), 47–54.

[5] W. A. Khan, O. D. Makinde, Z. H. Khan, Non-aligned MHD stagnation point flow of variable viscosity nanofluid past a stretching sheet with radiation heat, Int. J. Heat Mass Transfer, **96,** (2016), 525–534.

[6] A. C. Eringen, Simple micropolar fluids, Int. J. Eng. Sci., **2,** (1964), 205–217.

[7] A. C. Eringen, Theory of micropolar fluid, J. Math. Mech., **16,** (1966), 1-18.

[8] G. Lukaszewicz, Micropolar fluids: Theory and applications, Birkhauser, Basel, 1999.

[9] A. A. Mohammeadein, R. S. R. Gorla, Effects of transverse magnetic field on mixed convection in a micropolar fluid on a horizontal plate with vectored mass transfer, Acta. Mech., **118,** (1966), 1-12.

[10] S. R. Kasivishwanathan, M. V. A. Gandhi, class of exact solutions for the magnetohydrodynamic flow of a micropolar fluid, Int. J. Eng. Sci., **30,** (1992), 409–417.

[11] R. S. Agarwal, C. Dhanapal, Numerical solution of free convection micropolar fluid flow between two parallel porous vertical plates, Int. J. Eng. Sci., **26,** (1988), 1247–1255.

[12] R. Bhargava, L. Kumar, H. S. Takhar, Finite element solution of mixed convection micropolar flow driven by a porous stretching sheet, Int. J. Eng. Sci., **41,** (2003), 2161–2178.

[13] R. Nazar, N. Amin, D. Filip, I. Pop, Stagnation point flow of a micropolar fluid towards a stretching sheet, Int. J. Nonlinear Mech., **39,** (2004), 1227-1235.

[14] A. Ishak, R. Nazar, I. Pop, Magnetohydrodynamic flow of a micropolar fluid towards a stagnation point on a vertical surface, Comput. Math. Appl., **58,** (2008), 3188–3194.

[15] Z. Ziabakhsh, G. Domairry, Homotopy analysis solution of micropolar flow in a porous channel with high mass transfer, Adv. Theor. Appl. Mech., **2,** (2008), 79–94.

[16] D. Srinivasacharya, J. V. Ramanamurthy, D. Venugopalam , Unsteady Stokes flow of micropolar fluid between two parallel porous plates, Int. J. Eng. Sci.,**39,** (2001), 1557–1563.

[17] S. Nadeem, M. Sadaf, M. Rashid, A. S. Muhammad, Optimal and Numerical Solutions for an MHD MicropolarNanofluid between Rotating Horizontal Parallel Plates, Plos One, **6,** (2016), 4012–4016.

[18] S. Nadeem, Rashid Mehmood, S. Masood, Effects of transverse magnetic field on a rotating micropolar fluid between parallel plates with heat transfer, Journal of Magnetism and Magnetic Materials, **401,** (2016), 1006–1014.

[19] X. Q. WangArun, S. Mujumdar, A review on nanofluids, experiments and applications, Brazilian Journal of Chemical Engineering, **4,** (2008), 631–648.

[20] S. Goodman, Radiant-heat transfer between nongray parallel plates, J. of Research of the National Bureau of Standards, **58,** (1957), 27–32.

[21] A. K. Borkakoti, A. Bharali, Hydromagnetic flow and heat transfer between two horizontal plates, the lower plate is a stretching sheet, Q. Appl. Math., **41,** (1983), 461–467.

[22] H. D. Attia, N. B. Kotb, MHD Flow Between Parallel Plates with Heat transfer, Acta Mechanica, **117,** (1996), 215–220.

[23] M. Sheikholeslami, D. D. Ganji, Three dimensional heat and mass transfer in a rotating system using nanofluid, Powder Technology, **253,** (2014), 789–796.

[24] M. Sheikholeslami, H. M. Hatami, D. D. Ganji, Nanofluid flow and heat transfer in a rotating system in the presence of a magnetic field, Journal of Molecular Liquids, **190,** (2014), 112–120.

[25] M. Sheikholeslami, M. M. Rashidi, F. Firouzi, B. R. Houman, G. Domairry, The steady nanofluid flow between parallel plates considering thermophoresis and Brownian effects., Journal of King Saud University Science, **4,** (2015), 380-389.

[26] M. Sheikholeslami, D. D. Ganji, M. Y. Javed, R. Ellahi, Effect of thermal radiation on magnetohydrodynamics nanofluid flow and heat transfer by means of two-phase model, Journal of Magnetism and Magnetic Materials, **374,** (2015), 36–43.

[27] M. Sheikholeslami, Influence of magnetic field on nanofluid free convection in an open porous cavity by means of Lattice Boltzmann method, J. of Molecular Liquids, **234,** (2017), 364.

[28] M. Sheikholeslami, Magnetic field influence on nanofluid thermal radiation in a cavity with tilted elliptic inner cylinder, J. of Molecular Liquids, **229,** (2017), 137–147.

[29] M. Sheikholeslami, Magnetohydrodynamicnanofluid forced convection in a porous lid driven cubic cavity using Lattice Boltzmann method, J. of Molecular Liquids, **231,** (2017), 555–565.

[30] M. Sheikholeslami, Numerical simulation of magnetic nanofluid natural convection in porous media, Physics Letters A, **381** (2017), 494.

[31] M. Sheikholeslami, Numerical study of heat transfer enhancement in a pipe filled with porous media by axisymmetric TLB model based on GPU, Eur. Phys. J. Plus, **129,** (2014), 248.

[32] M. Sheikholeslam, CVFEM for magnetic nanofluid convective heat transfer in a porous curved enclosure, Eur. Phys. J. Plus, **131,** (2016), 413.

[33] M. Sheikholeslami, CuO-water nanofluid free convection in a porous cavity considering Darcy law, Eur. Phys. J. Plus, **132,** (2017), 55.

[34] M. Mahmoodi, S. Kandelousi, Application of DTM for kerosene-alumina nanofluid flow and heat transfer between two rotating plates, Eur. Phys. J. Plus, **130,** (2015), 142.

[35] M. S. Tauseef, Z. Ali, K. Z. Khan, N. Ahmed, On heat and mass transfer analysis of the flow of a nanofluid between rotating parallel plates, Aerospace Science and Technology, 2015.

[36] H. B. Rokni, D. M. Alsaad, P. Valipour, Electrohydrodynamicnanofluid flow and heat transfer between two plates, Journal of Molecular Liquids, **216,** (2016), 583–589.

[37] Geoffrey S. Taylor, Experiments with rotating fluids, Proc. Roy. London A, **100,** (1921), 114–121.

[38] H. P. Greenspan, The theory of rotating fluid, Cambridge University Press, 1968.

[39] K. Vajravelua, B. V. R. Kumar, Analytical and numerical solutions of a coupled non-linear system arising in a three-dimensional rotating flow, International Journal of Non-Linear Mechanics, **39,** (2004), 13–24.

[40] T. Hayat, M. Khursheed, M. Farooq, A. M. Alsaedi, Squeezed flow subject to CattaneoChristov heat flux and rotating frame, Journal of Molecular Liquids, **220,** (2016), 216–222.

[41] T. Hayat, S. Qayyum, M. Imtiaz, A. M. Alsaedi, Three-dimensional rotating flow of Jeffrey fluid for Cattaneo-Christov heat flux Model, AIP Advances, **6,** (2016), 1–11.